Performance enhancements in poly(vinylidene fluoride)-based piezoelectric films prepared by the extrusion-casting process

Chao Zhang[1] , Wei Wei[1], Huajun Sun[1,2,*], and Quanyao Zhu[1,*]

[1] *School of Materials Science and Engineering, Wuhan University of Technology, Wuhan 430070, People's Republic of China*
[2] *State Key Laboratory of Silicate Materials for Architectures, Wuhan University of Technology, Wuhan 430070, People's Republic of China*

ABSTRACT

The extrusion-casting process can realize large-area and continuous preparation of polymer-based films. In this paper, five different types of polyvinylidene fluoride (PVDF)-based piezoelectric films: PVDF, PVDF/PZT, PVDF/PZT@105, PVDF/PZT/BNNS and PVDF/PZT@105/BNNS were prepared by the extrusion-casting process. The mechanical, dielectric, thermal conductivity and piezoelectric properties were studied. It is found that PZT particles can well improve the dielectric performance and also the mechanical stability under variable temperature conditions. PZT powders modified by titanate coupling reagent (UP-105) can further improve the performance of the PVDF/PZT@105 films by improving the combination and dispersion of organic and inorganic phases. The addition of boron nitride nanosheets (BNNS) can improve the thermal conductivity of the films and the breakdown strength. The piezoelectric coefficient (d_{33}) of PVDF/PZT@105/BNNS composite film can reach 21pC/N, compared with the neat PVDF film (4pC/N) and PZT/PVDF (9pC/N) film realizing great improvement.

1 Introduction

Poly(vinylidene fluoride) (PVDF) films are widely applied as flexible piezoelectric sensors, soft robotics, energy harvesters and actuators [1–11] for they have lightweight, flexibility, superior mechanical properties, electrical breakdown strength, ferroelectricity and piezoelectricity [12–17]. Also, there exist many limitations such as low dielectric permittivity (ε), nonpolar phase in normal condition. To overcome these shortcomings, ceramics with high ε have been thought of comprising them with PVDF, leading to a combine of flexibility, high dielectric breakdown and high dielectric constant [18–22]. Now, 0–3 type PVDF/PZT piezoelectric composites are most exploited by the researchers for they have super properties [23–28]. However, there are many challenges such as the aggregation of fillers [29], poor

compatibility between the PVDF matrix and PZT fillers. To solve these problems, core–shell structure is proposed by researchers [18, 30, 31].

In order to keep the film flexible, the content of ceramic particles must be kept in a low range. However, it could not get good piezoelectric property when the content of ceramic particles is low, as it is difficult to achieve effective polarization of ceramic particles when the polarization voltage is small, leading to a poor piezoelectric performance. Therefore, high temperature and electric field are needed to effectively polarize the piezoelectric ceramic particles. How to improve the breakdown strength of the films and realize the effective polarization of ceramic particles is key to prepare the flexible films with excellent piezoelectric property.

In dielectric polymers, high dielectric loss will cause heat, leading to decline of the mechanical and electrical properties. The increase in temperature will lead to the variation of modulus of the polymer-based material, leading to the decrease of breakdown strength. Hence, how to increase thermal conductivity (TC) and decrease the conduction loss should be taken into consideration. To achieve high TC, many researchers have focused on fillers [32], such as BN [33], BNNS [20, 34, 35], graphene [36, 37], carbon nanotubes [38], etc. [39].

Currently, the laboratories generally adopt casting process to prepare PVDF-based films [40–43], which has the following disadvantages: (1) It is hard to get good density because a large number of solvents are used in the preparation process; (2) the preparation efficiency is low, and it is difficult to realize mass production; and (3) large-area films are difficult to prepare.

The extrusion-casting process can produce large-area, good density polymer films, which has been widely used in the preparation of polyethylene (PE), thermoplastic polyurethane (TPU), and so on. But is rarely reported in the preparation of PVDF/PZT composite piezoelectric films. In this work, we firstly prepared neat PVDF films by the extrusion-casting process, then PVDF/PZT composite films were prepared by adding 15wt% PZT piezoelectric ceramic particles. To further enhance the dispersion and combinability of PVDF and PZT in the films, titanate coupling agent (UP-105) was used to modify the surface of PZT, the film was labeled as PVDF/PZT@105. Furthermore, for improving the thermal conductivity (TC) and its breakdown strength at high temperature, we added 5wt% boron nitride nanometer sheet (BNNS) as the filling material to prepare PVDF/PZT/BNNS ternary piezoelectric films. The ternary film prepared by PZT@105 (modified by UP-105) was labeled as PVDF/PZT@105/BNNS. The mechanical and electrical performances of the five types films are studied, and the d_{33} of PVDF/PZT@105/BNNS film can reach 21pC/N.

2 Experimental

2.1 Raw materials

Poly(vinylidene fluoride) (PVDF) powders were purchased from Shandong Huaxia Shenzhou New Materials Co., Ltd., commercially available PZT-5H powders (Jude Electronic Technology Co., Ltd., China, Shandong, China, d_{33} = 590 pC/N, density = 7.6 g/cm^3) were used as fillers, commercial BNNS powders were obtained from Shanghai Chaowei Nanotechnology Co. Ltd., and titanate coupling agent (UP-105) was obtained from Nanjing Youpu Chemical Co. Ltd.

2.2 Preparation of different films

Five different kinds of films were prepared by an extrusion-casting-drawing-line equipment. The flat and dense films were obtained by adjusting the process parameters. Granular PVDF materials were used for preparing neat PVDF films with a thickness of about 50–100 μm. For PVDF/PZT composite films, PVDF powders and PZT powders (with a mass ratio of 85:15) were first added to a ball mill pot containing a certain amount of alcohol, then mixed on the ball mill for 6 h, and afterward dried in a blast dryer. The composite powders were extruded at 250 °C, the thickness of films are about 60–100 μm. Then the PZT powders were modified by UP-105 with an amount of about 0.8wt%. PVDF/PZT@105 films were prepared by the same process with a thickness of about 60–100 μm. The ternary PVDF/PZT/BNNS (PVDF/PZT/BNNS = 85:15:5, mass ratio) films were prepared by the same process with a thickness of about 60–100 μm. At last, PVDF/PZT@105/BNNS composite films were prepared by modified PZT@105 powders with a thickness of about 60-100 μm.

2.3 Characterization

Transmission electron micrographs of the fillers were tested by a high-resolution transmission electron microscopy (HRTEM, JEM-2100F, Japanese Electronics, China). FTIR spectra were recorded on the infrared spectrometer (NICOLET-IS50, Thermo Fisher, USA). The mechanical properties test response of samples was tested by a dynamic mechanical analyzer (DMA) (RSA-G2 Solids Analyzer, TA Instruments, USA). The crystal structure was measured by a X-ray diffraction (XRD, Bruker D8 Advanced, Germany). The morphology and element mapping test were characterized by scanning electron microscopy (FESEM, S-4800, Hitachi, Tokyo, Japan). For electric measurement, the films were coated on the two surfaces with silver electrodes (Φ6mm) using a coating method. The frequency dependencies of dielectric properties were measured with a NOVOCONTROL test system (Concept 80, Germany). Electric breakdown tests were carried out with a Withstand Voltage Test System (7474, EXTECH ELECTRONICS CO., LTD.), and the samples were immersed in silicon oil. The thermal conductivity was measured by hot disk instrument (DTC-25, TA Corporation, USA), and the films were cut into round pieces (Φ50 mm). The piezoelectric coefficients were measured using a static tester (Piezo Test; Acoustic, Chinese Academy of Sciences).

3 Results and discussion

The transmission electron micrograph of the modified PZT is shown in Fig. 1a, as can be seen that the thickness of the coupling agent is about a few nanometers. The infrared spectroscopy of the modified PZT fillers phase is shown in Fig. 1b. It can be seen that the absorption peaks of the treated PZT powder appear at 2921 cm^{-1} and 2852 cm^{-1}, corresponding to the characteristic absorption peaks of CH_3 and CH_2 of titanate coupling agent.

The microcosmic morphology can be observed from Fig. 2, showing that the PZT/PZT film has poor density with many defects and voidage in the interface (Fig. 2b). However, this phenomenon largely disappeared in the PVDF/PZT@105 film, showing that the surface modification of PZT by UP-105 greatly improves the dispersion and combination of PVDF and PZT [44, 45]. As indicated in Fig. 2d,
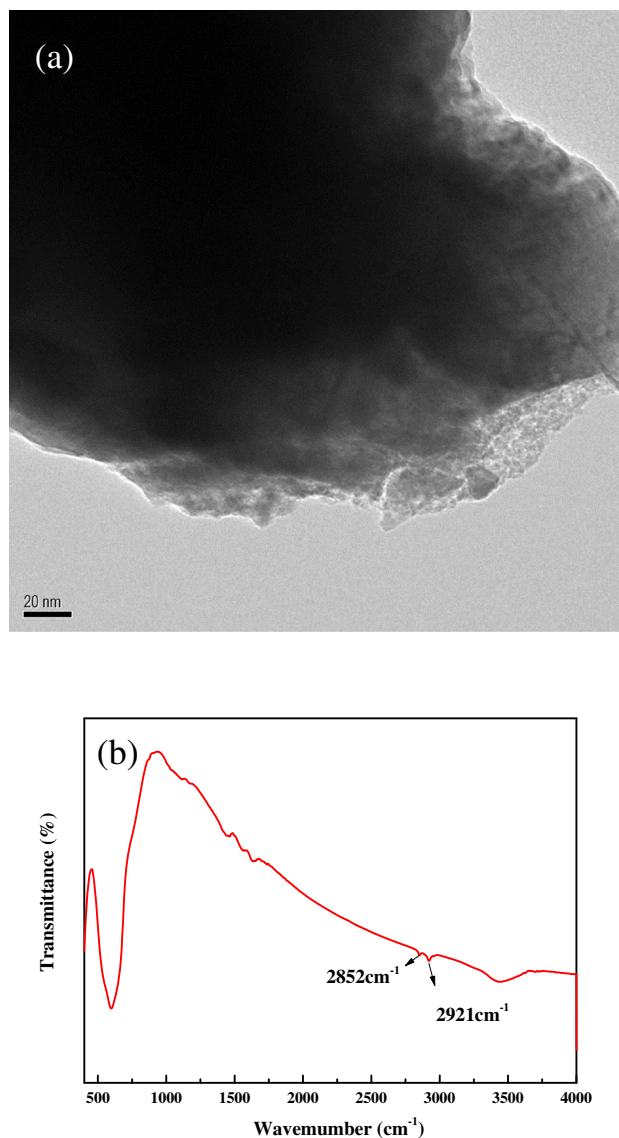

Fig. 1 The transmission electron micrograph (**a**) and infrared spectroscopy (**b**) of the modified PZT

BNNS particles are well dispersed in PVDF/PZT/BNNS film which means the polar B-N bonds could well interact with the polar PVDF matrix [20]. The reason for adding 15% PZT is to maintain the flexibility of the films and improve the electrical properties as much as possible, because when the addition amount is too large, the films are difficult to densification, and exist larger brittleness. An element mapping of PVDF/PZT@105/BNNS film is shown in Fig. 3. The distribution of elements of different substances in the film is confirmed.

XRD spectra of neat PVDF, PVDF/PZT, PVDF/PZT@105, PVDF/PZT/BNNS and PVDF/PZT@105/

Fig. 2 SEM of PVDF-based composite films: **a** neat PVDF film, **b** PZT/PZT film, **c** PZT/PZT@105 film, **d** PVDF/PZT/BNNS film, **e** PVDF/PZT@105 /BNNS film
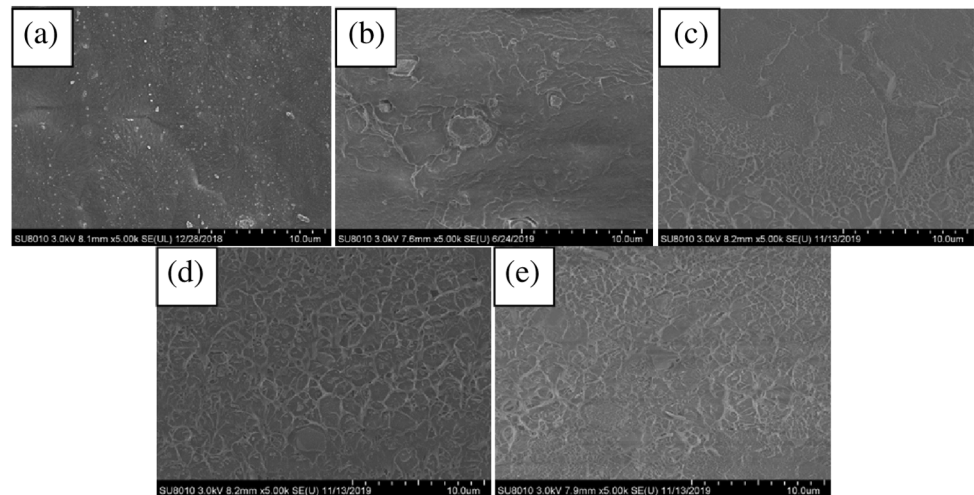
BNNS films are presented in Fig. 4. The neat PVDF film shows an α crystal form in majority (18.6°, 20.1°, 26.9°) [20]. The main reason is that when the film is prepared by the extrusion molding process, the temperature is as high as 250 °C. When the polymer melt is extruded, the molten state of PVDF changes sharply from high temperature to low temperature. PVDF is easy to form α phase after cooling down in high temperature. We can see that the diffraction signals of BNNS (26.8°, 50.1°) [20] and PZT (21–22.5°, 43–45°) [27, 46] could be identified clearly.

3.1 Study on mechanical properties

When piezoelectric films are used as sensing materials, they will deform under the tension or pressure. The deformation needs to be in the elastic deformation interval; otherwise, it cannot be restored to its original state. Generally speaking, at the early stage of stretching, the stress and strain of the polymer-based films basically change linearly, stay in the elastic interval. When the films continue being stretched, the yield points appeared, the range of the
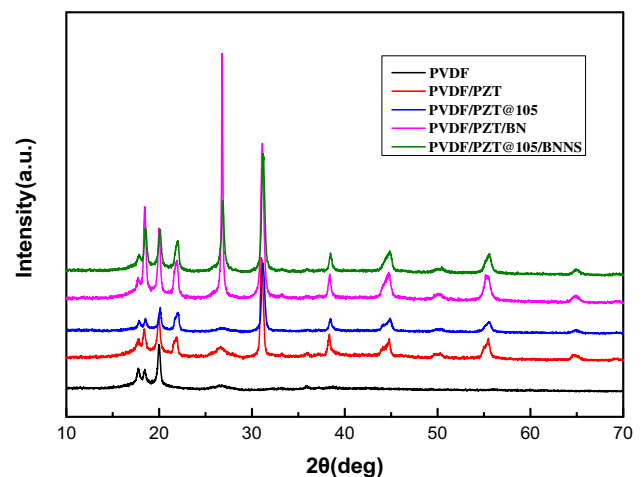

Fig. 4 XRD spectra of the PVDF-based films

elastic interval can be determined according to the position of the yield point. Figure 5 shows the tensile properties of different films at room temperature (The ratio of length to width of the film is 5:1, and the tensile rate is 0.5 mm/s). It can be seen that the tensile strength approximate 60 MPa with a maximum strain of 10% in neat PVDF film. The PVDF/PZT film

Fig. 3 Element mapping of PVDF/PZT@105/BNNS film
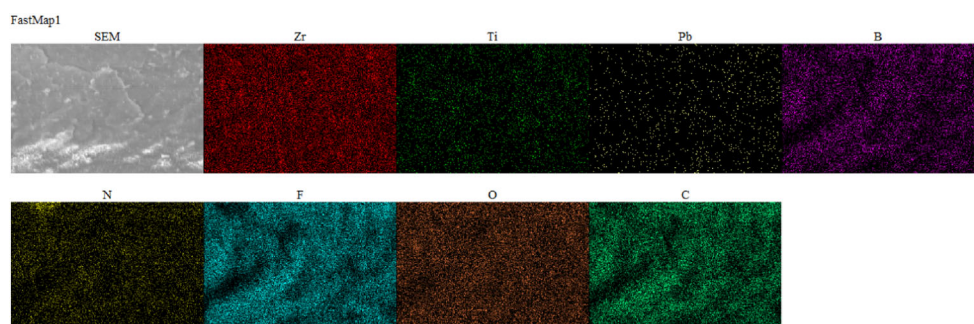
has reduced strength (30 MPa) and stretchability (5%) which is related to the awful dispersion of PZT and the poor combination of the two terms which also can be observed in Fig. 2b. The PVDF/PZT@105 film exhibits higher strength (35 MPa) and ductility compared with PVDF/PZT film mainly due to its uniform distribution, realizing an effective load transfer. It shows that the UP-105 shell enhances the dispersion state and compatibility of PZT@105 in the PVDF matrix. Adding BNNS further increases the tensile strength of the film, but does not significantly affect the elastic interval, the possible reason is that the tiny boron nitride fills the tiny holes in the PVDF/PZT/BNNS film, increasing its density, which can also be seen in the PVDF/PZT@105/BNNS film.

Temperature is an important factor in the application of elastomers, and changes in temperature often lead to vary in mechanical and electrical properties. The storage modulus curves depending on temperature of PVDF-based films are shown in Fig. 6. (The
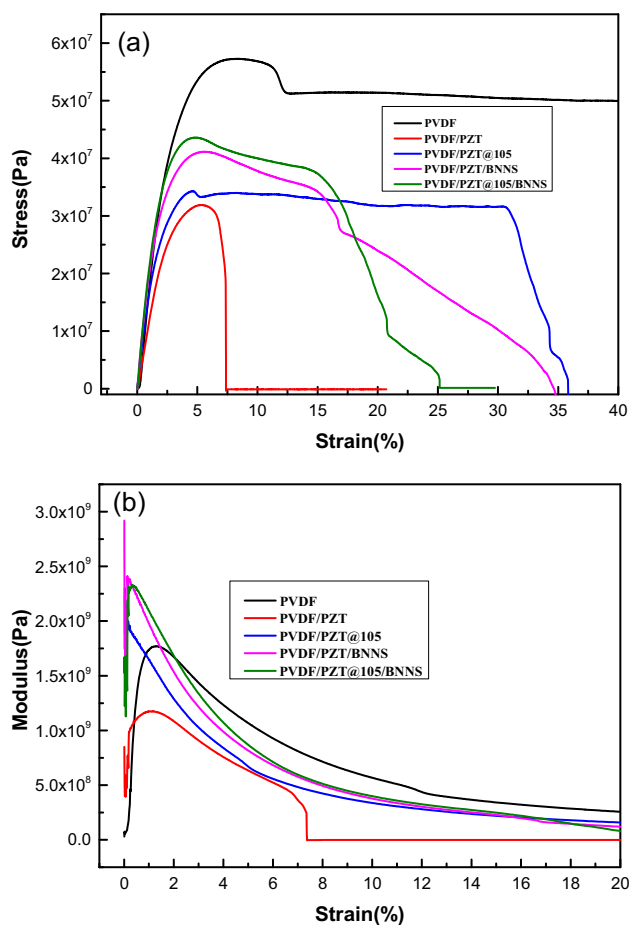
ratio of length to width of the film is 5:2, the amplitude deformation is 0.2%, and oscillation frequency is 2 Hz.) Generally speaking, the application temperature range of PVDF-based films as sensing materials is between 25 and 40 °C. By comparing the storage modulus of PVDF-based films in this interval, we can see that, PVDF is very sensitive to temperature, the storage modulus decreases sharply as temperature increases. PVDF-based composite films show enhanced temperature stability, and the decline magnitude of the storage modulus has been greatly reduced. It is probably associable the introduction of the PZT and BNNS powders that prohibiting the motions of the PVDF molecular. The change of modulus can seriously affect the force-electric conversion effect, so PVDF-based composite films have advantages as elastomers than neat PVDF films.

3.2 Study on dielectric properties

The dielectric properties mainly containing dielectric constant (ε) and dielectric loss ($\tan\delta$) are very important parameters [20]. Figure 7 compares the dielectric behavior of PVDF-based films depends on frequency (25 °C). In all the films, dielectric constant decreases with the increases in frequency because the space charge polarization disappears replaced by the dipolar polarization. PVDF/PZT composite film has a higher ε (22) than neat PVDF film (11) due to the high dielectric constant of PZT fillers [35, 36]. The dielectric constant of the PVDF/PZT@105 film decreases compared with unmodified one; this is mainly because of the shielding effect of UP-105 on

Fig. 5 Tensile properties at room temperature (25 °C): a stress–strain curves; b modulus–strain curves
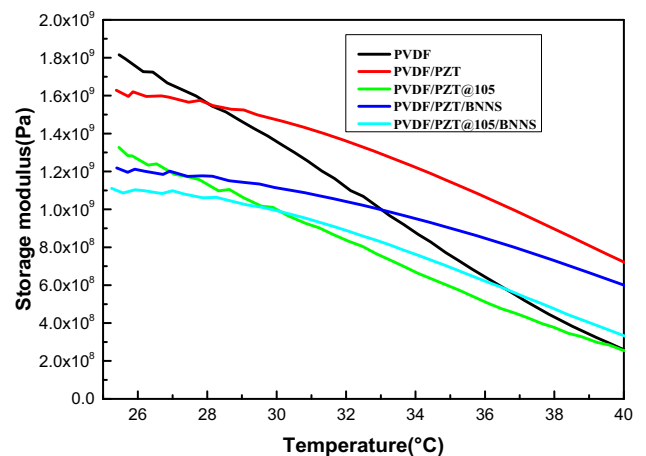

Fig. 6 Storage modulus–temperature curves of different types of PVDF-based films

the PZT particles [40, 41]. The dielectric loss decreases rapidly with frequency which can be seen in Fig. 7b because the charge carrier is suppressed with
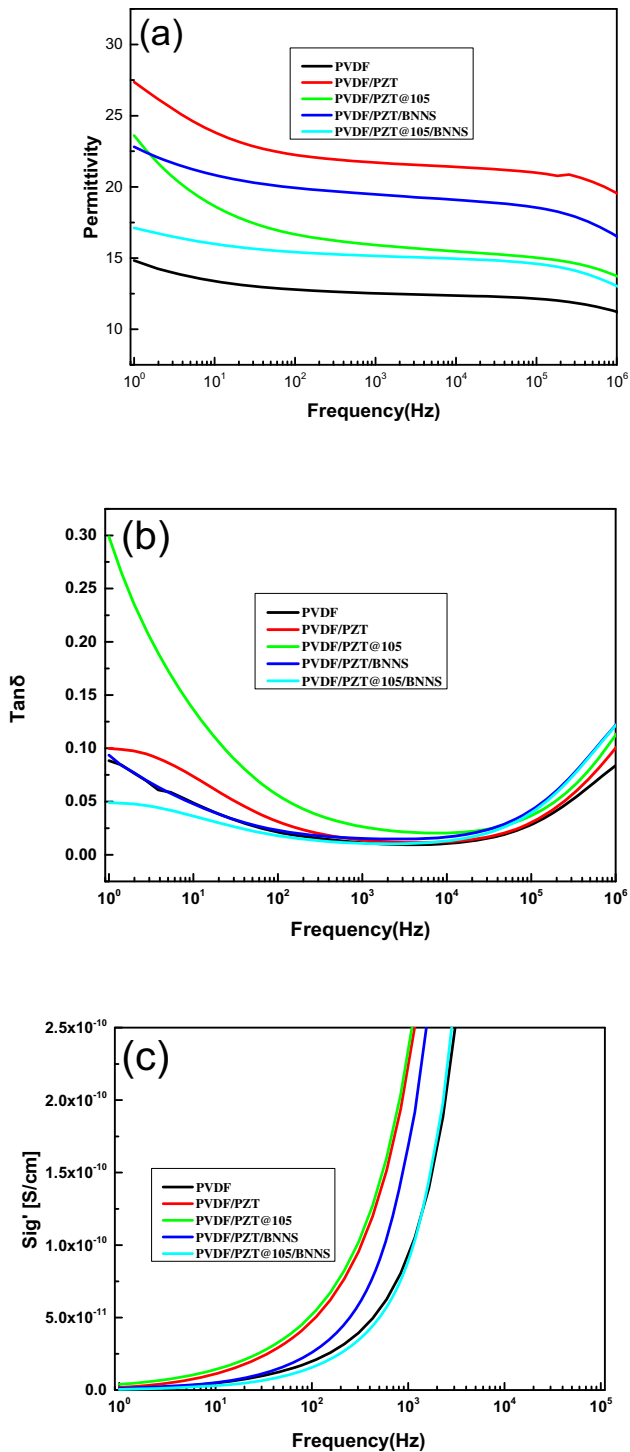
an increase in frequency and interfacial polarization cannot change with frequency immediately. The dielectric loss increases again at higher frequencies ($> 10^4$ Hz) because the dipole reversal lags behind the change of electric field [31]. The alternating current (AC) conductivities as a function of frequency are presented in Fig. 7c. The conductivity is decreased by adding 5wt% BNNS, due to the good insulating performance of BNNS. The introduction of PZT will cause increased AC conductivity, while could be well eliminated by adding 5wt% BNNS, which can be seen in the PVDF/PZT@105/BNNS film.

3.3 Heat conduction performance

The thermal conduction also needs to be attention in the application. If the heat induced by the dielectric loss and leak conductance accumulates continuously, the films may be deteriorated [30–32, 37–39]. Figure 8 shows the thermal conducting (TC) property of different films in a through-plane way. The TC of neat PVDF is 0.14 W/mK, while the PVDF/PZT@105/BNNS film can reach 0.18 W/mK, approximately 30% enhancement. High thermal conductivity is due to the high TC of BNNS and well linkage between BNNS and PVDF matrix.
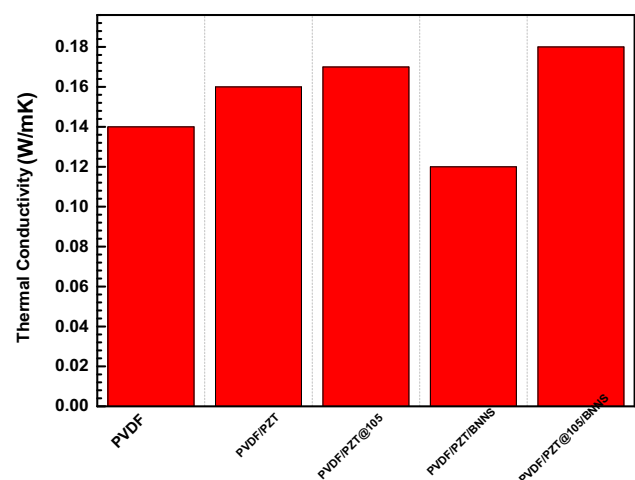

Fig. 7 Dielectric properties of different types of PVDF-based films: **a** dielectric constant–frequency curves, **b** tanδ–frequency curves, **c** conductivity–frequency curves

Fig. 8 Thermal properties of composite films: thermal conductivity through-plane

3.4 Study on the breakdown strength of PVDF-based composite films

Breakdown strength (E_b) is a crucial factor of PVDF-based composite films. We use Weibull statistic to analyze E_b as described in Eq. 1 [20].

$$F(E) = 1 - \exp\left[-\left(\frac{E}{\alpha}\right)^\beta\right] \qquad (1)$$

In this equation, $F(E)$ is the cumulative probability of electric failure, β evaluates the scatter of data, E represents the breakdown electric field, α is the electric field strength for the sample to breakdown at a 63% probability. The results are presented in Fig. 9. By comparing the breakdown strength at room temperature (25 °C), we can see that neat PVDF film has the highest value which can reach 303 kV/mm, while the breakdown strength of PVDF/PZT film drops to 210 kV/mm. These results due to the low breakdown strength of PZT, the electric field distortion effect and defects come from PZT agglomeration. The E_b of the PVDF/PZT@105 film reaches 251 kV/mm which is 19.5% higher than PVDF/PZT film; it is due to the improved dispersion and good combination of PZT in PVDF matrix. The comparison between PVDF/PZT/BNNS and PVDF/PZT films shows that the addition of BNNS fillers enhances the breakdown strength to 234 kV/mm, mainly because BNNS fillers improve the density of the film, which can be seen from Fig. 2d.

The E_b of neat PVDF film decreases from 303 kV/mm to 111 kV/mm with the temperature increases from 25 to 100 °C (Fig. 9a), while the PVDF/PZT@105/BNNS film has the best breakdown strength from 60 to 100 °C. The addition of BNNS leads to remarkably enhanced E_b at high temperature, mainly because: (1) The excellent insulating performance of BNNS lowers the dielectric loss (Fig. 5b); (2) High TC of the film (Fig. 8); (3) BNNS fillers improve the breakdown current, effectively avoid the concentration of electrical charges, and prevent the growth of electric tree. The breakdown current of different types of films is shown in Fig. 10; we can see that the breakdown current increases with the temperature increases. The films with BNNS have greater resistance to breakdown current at higher temperature; this is mainly because BNNS can effectively disperse the free charge under high electric field and avoid the concentration of the electrical
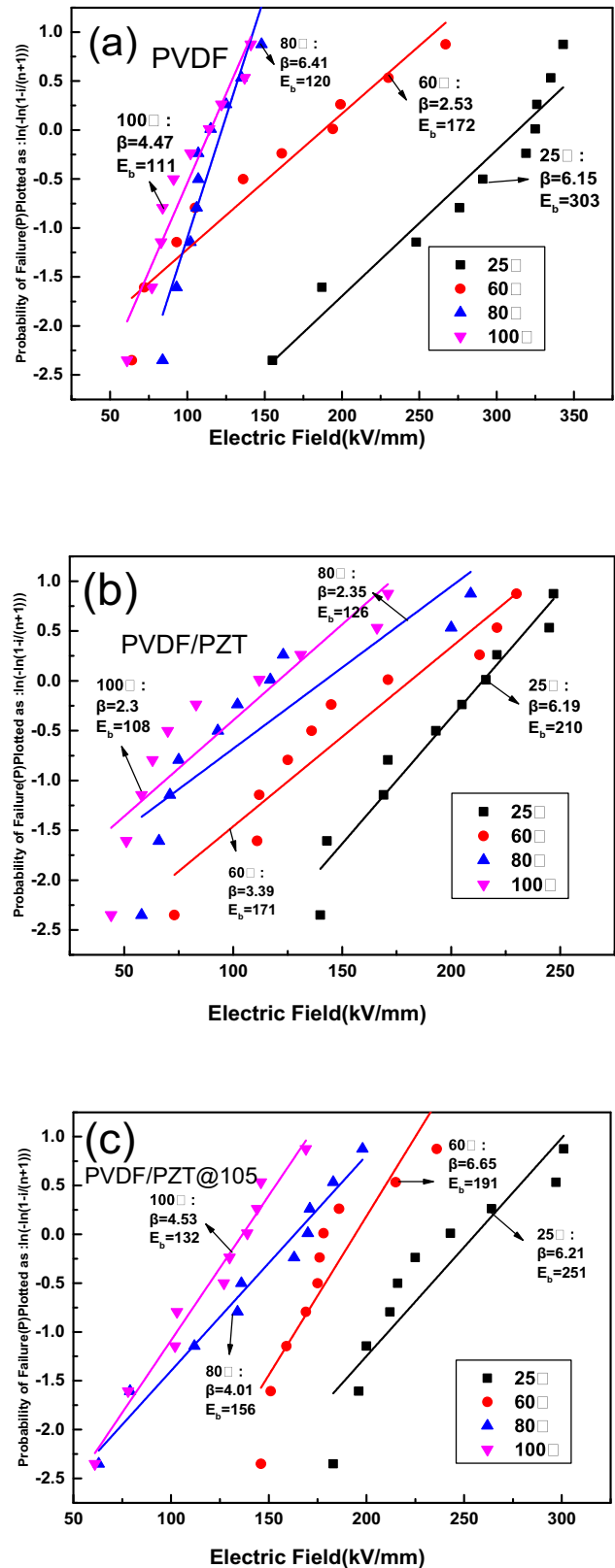

Fig. 9 Weibull distribution and breakdown strength of PVDF-based composite films with various temperature
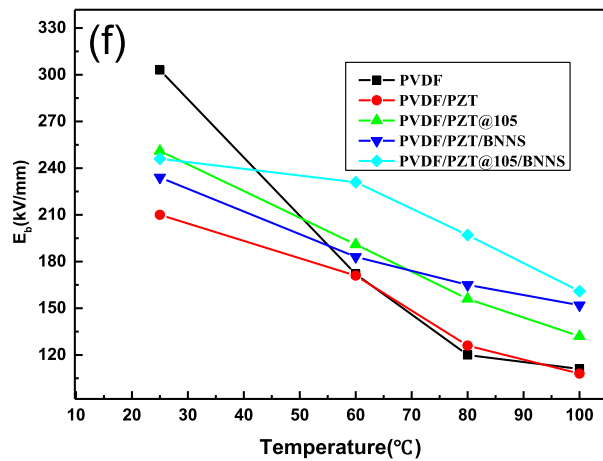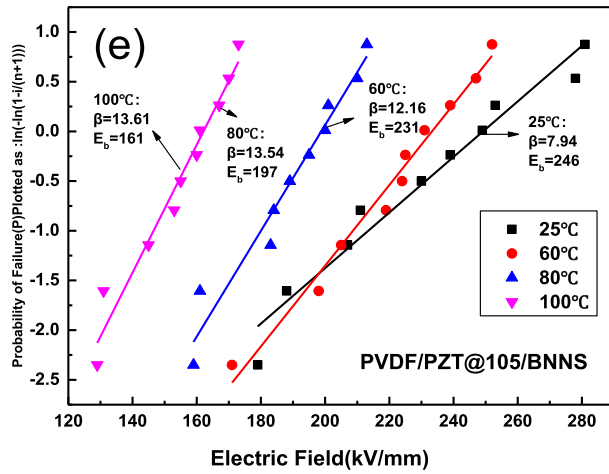
Fig. 10 The breakdown current of PVDF-based composite films varies with temperatures

3.5 Piezoelectric properties

Figure 11 shows the piezoelectric coefficient (d_{33}) of different films. The neat PVDF film shows the d_{33} value as 4pC/N, whereas it is increased to 9pC/N of the PVDF/PZT film. The PVDF/PZT@105/BNNS composite film has the largest d_{33} which can reach 21pC/N. The increased d_{33} may be attributed to the good polarization progress, because this type of film has the highest breakdown field and it can be polarized under high electric field intensity.
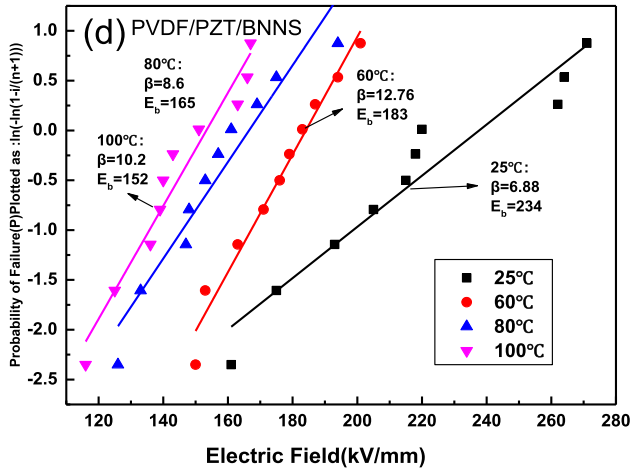

Fig. 9 continued

charges, thus preventing the electron avalanche effect; (4) Coupled with the higher Young's modulus (Fig. 5b) which impedes the electromechanical breakdown [39].
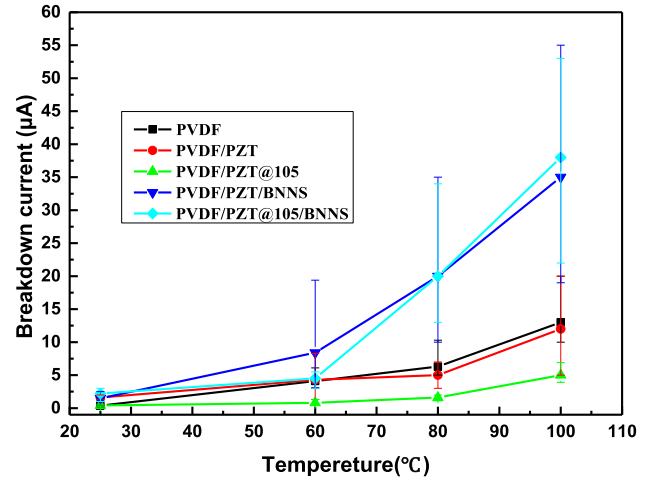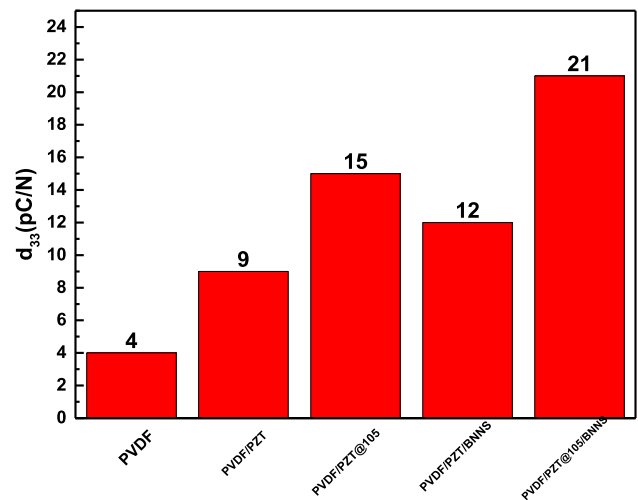

Fig. 11 d_{33} of PVDF-based composite films

4 Conclusion

This study has demonstrated a technique for processing large-area of PVDF-based composite films meanwhile significantly increasing the d_{33} by the extrusion-casting process. The surface modification of PZT particles by titanate coupling agent (UP-105) improves dispersion in PVDF matrix and compatibility with PVDF matrix. The addition of PZT@105 and BNNS improves the mechanical stability of the films under various temperature. BNNS improves the TC (longitudinal) of the films and also the breakdown strength of the film at high temperature, which is conducive to improve the stability of the film. The d_{33} of PVDF/PZT@105/BNNS composite film could reach 21pC/N because it can be polarized under higher electric field intensity and it has higher E_b.

Acknowledgements

References

1. J. Yan, M. Liu, Y.G. Jeong, W. Kang, L. Li, Y. Zhao, N. Deng, B. Cheng, G. Yang, Performance enhancements in poly(vinylidene fluoride)-based piezoelectric nanogenerators for efficient energy harvesting. Nano Energy **56**, 662–692 (2019)

2. K.Y. Cho, H. Park, H.-J. Kim, X.H. Do, C.M. Koo, S.S. Hwang, H.G. Yoon, K.-Y. Baek, Highly enhanced electromechanical properties of PVDF-TrFE/SWCNT nanocomposites using an efficient polymer compatibilizer. Compos. Sci. Technol. **157**, 21–29 (2018)

3. K.S. Ramadan, D. Sameoto, S. Evoy, A review of piezoelectric polymers as functional materials for electromechanical transducers. Smart Mater. Struct. **23**(3), 033001 (2014)

4. L. Jin, S. Ma, W. Deng, C. Yan, T. Yang, X. Chu, G. Tian, D. Xiong, J. Lu, W. Yang, Polarization-free high-crystallization β-PVDF piezoelectric nanogenerator toward self-powered 3D acceleration sensor. Nano Energy **50**, 632–638 (2018)

5. X. Huang, B. Sun, Y. Zhu, S. Li, P. Jiang, High-k polymer nanocomposites with 1D filler for dielectric and energy storage applications. Prog. Mater Sci. **100**, 187–225 (2019)

6. R. Shankar, T.K. Ghosh, R.J. Spontak, Dielectric elastomers as next-generation polymeric actuators. Soft Matter **3**(9), 1116–1129 (2007)

7. V.F. Cardoso, T. Knoll, T. Velten, L. Rebouta, P.M. Mendes, S. Lanceros-Méndez, G. Minas, Polymer-based acoustic streaming for improving mixing and reaction times in microfluidic applications. RSC Adv. **4**(9), 4292–4300 (2014)

8. S.O. Catarino, L.R. Silva, P.M. Mendes, J.M. Miranda, S. Lanceros-Mendez, G. Minas, Piezoelectric actuators for acoustic mixing in microfluidic devices-Numerical prediction and experimental validation of heat and mass transport. Sens. Actuators B **205**, 206–214 (2014)

9. C. Ribeiro, C.M. Costa, D.M. Correia, J. Nunes-Pereira, J. Oliveira, P. Martins, R. Goncalves, V.F. Cardoso, S. Lanceros-Mendez, Electroactive poly(vinylidene fluoride)-based structures for advanced applications. Nat Protoc. **13**(4), 681–704 (2018)

10. J.-H.Bae, S.-H. Chang, PVDF-based ferroelectric polymers and dielectric elastomers for sensor and actuator applications: a review. Funct. Compos. Struct. **1**, 012003 (2019).

11. W. Xia, Z. Zhang, PVDF-based dielectric polymers and their applications in electronic materials. IET Nanodielectr. **1**(1), 17–31 (2018)

12. F. Liu, N.A. Hashim, Y. Liu, M.R.M. Abed, K. Li, Progress in the production and modification of PVDF membranes. J. Membr. Sci. **375**(1–2), 1–27 (2011)

13. J. Chen, Y. Wang, Q. Yuan, X. Xu, Y. Niu, Q. Wang, H. Wang, Multilayered ferroelectric polymer films incorporating low-dielectric-constant components for concurrent enhancement of energy density and charge–discharge efficiency. Nano Energy **54**, 288–296 (2018)

14. J. Fu, Y. Hou, X. Gao, M. Zheng, M. Zhu, Highly durable piezoelectric energy harvester based on a PVDF flexible nanocomposite filled with oriented $BaTi_2O_5$ nanorods with high power density. Nano Energy **52**, 391–401 (2018)

15. L. Zhang, Z. Liu, X. Lu, G. Yang, X. Zhang, Z.Y. Cheng, Nano-clip based composites with a low percolation threshold and high dielectric constant. Nano Energy **26**, 550–557 (2016)

16. T. Soulestin, V. Ladmiral, F.D. Dos Santos, B. Améduri, Vinylidene fluoride- and trifluoroethylene-containing fluorinated electroactive copolymers How does chemistry impact properties? Progr. Polym. Sci. **72**, 16–60 (2017)

17. Y. Zhang, C. Zhang, Y. Feng, T. Zhang, Q. Chen, Q. Chi, L. Liu, G. Li, Y. Cui, X. Wang, Z. Dang, Q. Lei, Excellent energy storage performance and thermal property of polymer-based composite induced by multifunctional one-dimensional nanofibers oriented in-plane direction. Nano Energy **56**, 138–150 (2019)

18. K. Bi, M. Bi, Y. Hao, W. Luo, Z. Cai, X. Wang, Y. Huang, Ultrafine core-shell BaTiO$_3$@SiO$_2$ structures for nanocomposite capacitors with high energy density. Nano Energy **51**, 513–523 (2018)

19. S. Luo, J. Yu, S. Yu, R. Sun, L. Cao, W.-H. Liao, C.-P. Wong, Significantly Enhanced Electrostatic Energy Storage Performance of Flexible Polymer Composites by Introducing Highly Insulating-Ferroelectric Microhybrids as Fillers. Adv. Energy Mater. **9**, 1803204 (2019).

20. Y. Xie, J. Wang, Y. Yu, W. Jiang, Z. Zhang, Enhancing breakdown strength and energy storage performance of PVDF-based nanocomposites by adding exfoliated boron nitride. Appl. Surf. Sci. **440**, 1150–1158 (2018)

21. Z.-H. Shen, J.-J. Wang, Y. Lin, C.-W. Nan, L.-Q. Chen, Y. Shen, High-throughput phase-field design of high-energy-density polymer nanocomposites. Adv. Mater. **30**, 1704380 (2018).

22. Y. Jiang, X. Zhang, Z. Shen, X. Li, J. Yan, B.-W. Li, C.-W. Nan, Ultrahigh breakdown strength and improved energy density of polymer nanocomposites with gradient distribution of ceramic nanoparticles. Adv. Funct. Mater. **30**, 1906112 (2020).

23. P.-H. Cazorla, O. Fuchs, M. Cochet, S. Maubert, G. Le Rhun, Y. Fouillet, E. Defay, A low voltage silicon micro-pump based on piezoelectric thin films. Sens. Actuators A **250**, 35–39 (2016)

24. G. Chen, X. Lin, J. Li, J.G. Fisher, Y. Zhang, S. Huang, X. Cheng, Enhanced dielectric properties and discharged energy density of composite films using submicron PZT particles. Ceram. Int. **44**(13), 15331–15337 (2018)

25. V. Tiwari, G. Srivastava, Structural, dielectric and piezoelectric properties of 0–3 PZT/PVDF composites. Ceram. Int. **41**(6), 8008–8013 (2015)

26. S. Revathi, L.J. Kennedy, S.K.K. Basha, R. Padmanabhan, Synthesis, structural, optical and dielectric properties of nanostructured 0–3 PZT/PVDF composite films. J Nanosci Nanotechnol **18**(7), 4953–4962 (2018)

27. J. Pei, Z. Zhao, X. Li, H. Liu, R. Li, Effect of preparation techniques on structural and electrical properties of PZT/PVDF composites. Mater. Express **7**(3), 180–188 (2017)

28. R.L.B. de Freitas, W.K. Sakamoto, L.P.S. Freitas, F. Castro, A.P.L. Filho, C. Kitano, A.A. de Carvalho, Characterization of PZT/PVDF composite film as functional material. IEEE Sensors J. **18**(12), 5067–5072 (2018)

29. Q. Wu, D.-J. Xie, Y.-D. Zhang, Z.-M. Jia, H.-Z. Zhang, Mechanical properties and simulation of nanographene/polyvinylidene fluoride composite films. Compos. B Eng. **156**, 148–155 (2019)

30. M.-S. Zheng, Y.-T. Zheng, J.-W. Zha, Y. Yang, P. Han, Y.-Q. Wen, Z.-M. Dang, Improved dielectric, tensile and energy storage properties of surface rubberized BaTiO$_3$/polypropylene nanocomposites. Nano Energy **48**, 144–151 (2018)

31. S.Y.L. Zhang, S. Chen, D. Wang, B.-Z. Han, Z.M. Dang, Preparation and dielectric properties of core-shell structured Ag@polydopamine/poly(vinylidene fluoride) composites. Compos. Sci. Technol. **110**, 126–131 (2015)

32. L. Zhou, Y. Zhou, Y. Shi, T. Chen, T. Zou, D. Zhou, Q. Fu, Enhancing thermal stability of P(VDF-HFP) based nanocomposites with core-shell fillers for energy storage applications. Compos. Sci. Technol. **186**, 107934 (2020)

33. C. Xiao, Y. Tang, L. Chen, X. Zhang, K. Zheng, X. Tian, Preparation of highly thermally conductive epoxy resin composites via hollow boron nitride microbeads with segregated structure. Compos. A Appl. Sci. Manuf. **121**, 330–340 (2019)

34. C. Fu, C. Yan, L. Ren, X. Zeng, G. Du, R. Sun, J. Xu, C.-P. Wong, Improving thermal conductivity through welding boron nitride nanosheets onto silver nanowires via silver nanoparticles. Compos. Sci. Technol. **177**, 118–126 (2019)

35. J. Chen, X. Huang, B. Sun, P. Jiang, Highly thermally conductive yet electrically insulating polymer/boron nitride nanosheets nanocomposite films for improved thermal management capability. ACS Nano **13**(1), 337–345 (2018)

36. Y. Zhuang, K. Zheng, X. Cao, Q. Fan, G. Ye, J. Lu, J. Zhang, Y. Ma, Flexible graphene nanocomposites with simultaneous highly anisotropic thermal and electrical conductivities prepared by engineered graphene with flat morphology. ACS Nano **14**(9), 11733–11742 (2020)

37. X. Huang, C. Zhi, Y. Lin, H. Bao, G. Wu, P. Jiang, Y.-W. Mai, Thermal conductivity of graphene-based polymer nanocomposites. Mater. Sci. Eng. R **142**, 100577 (2020)

38. Z.-G. Wang, Y.-F. Huang, G.-Q. Zhang, H.-Q. Wang, J.-Z. Xu, J. Lei, L. Zhu, F. Gong, Z.-M. Li, Enhanced thermal conductivity of segregated poly(vinylidene fluoride) composites via forming hybrid conductive network of boron nitride and carbon nanotubes. Ind. Eng. Chem. Res. **57**, 10391–10397 (2018)

39. Q. Li, L. Chen, M.R. Gadinski, S. Zhang, G. Zhang, U. Li, E. Iagodkine, A. Haque, L.Q. Chen, N. Jackson, Q. Wang, Flexible high-temperature dielectric materials from polymer nanocomposites. Nature **523**, 576–579 (2015)

40. Y.S.H. Horibe, H. Oshiro, Y. Hosokawa, A. Kono, S. Takahashi, T. Nishiyama, Quantification of the solvent evaporation rate during the production of three PVDF crystalline structure types by solvent casting. Polym. J. **46**, 104–110 (2014)

41. S. Dash, R.N.P. Choudhary, M.N. Goswami, Enhanced dielectric and ferroelectric properties of PVDF-BiFeO$_3$ composites in 0–3 connectivity. J. Alloys Compd. **715**, 29–36 (2017)

42. B. Xie, Q. Zhang, L. Zhang, Y. Zhu, X. Guo, P. Fan, H. Zhang, Ultrahigh discharged energy density in polymer nanocomposites by designing linear/ferroelectric bilayer heterostructure. Nano Energy **54**, 437–446 (2018)

43. A. Pal, A. Sasmal, B. Manoj, D.S.D.P. Rao, A.K. Haldar, S. Sen, Enhancement in energy storage and piezoelectric performance of three phase (PZT/MWCNT/PVDF) composite. Mater. Chem. Phys. **244**, 122639 (2020)

44. Y. Zhang, J. Gao, H. Li, E. Wang, J. Zhang, L. Zhang, Effect of chelating polymer as chelating agent on the PZT/PVDF pyroelectric composites. J. Mater. Sci. **27**(11), 11733–11738 (2016)

45. R. Li, L. Zhang, Z. Shi, J. Pei, Effects of coupling agents on the structure and electrical properties of PZT-poly (vinylidene fluoride) composites. Appl. Sci. **6**(10), 282 (2016)

46. R. Li, J. Zhou, H. Liu, J. Pei, Effect of polymer matrix on the structure and electric properties of piezoelectric lead zirconatetitanate/polymer composites. Materials **10**(8), 945 (2017)